Electrochemomechanics of Electrodes in Li-Ion Batteries: A Review

Rong Xu
School of Mechanical Engineering,
Purdue University,
West Lafayette, IN 47906

Kejie Zhao[1]
School of Mechanical Engineering,
Purdue University,
West Lafayette, IN 47906
e-mail: kjzhao@purdue.edu

A Li-ion battery is a system that dynamically couples electrochemistry and mechanics. The electrochemical processes of Li insertion and extraction in the electrodes lead to a wealth of phenomena of mechanics, such as large deformation, plasticity, cavitation, fracture, and fatigue. Likewise, mechanics influences the thermodynamics and kinetics of interfacial reactions, ionic transport, and phase transformation of the electrodes. The emergence of high-capacity batteries particularly enriches the field of electrochemomechanics. This paper reviews recent observations on the intimate coupling between stresses and electrochemical processes, including diffusion-induced stresses, stress-regulated surface charge transfer, interfacial reactions, inhomogeneous growth of lithiated phases, instability of solid-state reaction front (SSRF), as well as lithiation-modulated plasticity and fracture in the electrodes. Most of the coupling effects are at the early stage of study and are to be better understood. We focus on the elaboration of these phenomena using schematic illustration. A deep understanding of the interactions between mechanics and electrochemistry and bridging these interdisciplinary fields can be truly rewarding in the development of resilient high-capacity batteries.
[DOI: 10.1115/1.4035310]

Keywords: Li-ion batteries, electrochemomechanics, stress, diffusion, reaction

1 Introduction

Li-ion batteries play a dominant role in the market of portable electronics and drive the commercialization of electric vehicles. Global efforts are being dedicated to develop batteries of high energy density, fast charging and power output, low cost, and safe operation [1–4]. The durability of mechanical strength and integrity over long-term cycles are important criteria in the selection of battery materials. For instance, mechanical degradation places an intrinsic drawback on most of the high-capacity electrodes because large volumetric expansion is inherent to the massive insertion of Li into the host materials [5–7]. The structural disintegrity impedes electron conduction and increases the thermal and ohmic resistances which could cause catastrophic failure of batteries [8]. Meanwhile, the mechanical deformation of active material interferes with the stability of solid electrolyte interface (SEI) which results in a persistent decrease of cyclic efficiency [9]. Many clever designs in recent years, for example, by creating open spaces to accommodate volumetric swelling [10–15], compositing active phase and inactive components [16–18], depositing metal oxides surface coating [19,20], constructing hierarchal structures [21,22], or manipulating geometries and patterns at the nanoscale [23–25], have helped mitigate the mechanical failure of batteries. Nevertheless, maintaining the mechanical resilience remains a grand challenge for high-capacity electrodes and mechanics perspectives provide important insight in the course of developing reliable batteries [26,27].

On the side of fundamental mechanics, Li-ion batteries provide an excellent platform to study the intimate coupling between mechanics and electrochemistry. The electrochemical process of Li insertion and extraction induces rich phenomena of elemental mechanics, such as large elastoplastic deformation [28,29], cavitation [30,31], reactive plasticity [32–34], and corrosive fracture [35]. Meanwhile, mechanical stresses modulate the thermodynamics and kinetics of ionic transport, surface charge transfer, interfacial reaction, and phase transition of materials [36–38]. While the mechanical deformation and failure in the cycles of batteries are well known [10,26,39,40], the influences of stresses on the electrochemical reactions are less obvious and are much less studied. In fact, for a system involving multiphysical processes, a conventional wisdom is that "chemistry always win" simply because the energy scales in the chemical reactions are usually orders of magnitude higher than the mechanical energies [41]. Li-ion batteries might be an exception in that the chemical driving force (bonding energy) in the lithiation/delithiation reactions is relatively weak in order to maintain a good cyclability, while the mechanical deformation and stresses are usually significant that leverages the mechanical energy to a level comparable with the chemical energies [42–46]. The pursue of electrochemomechanics in the example system of Li-ion batteries may provide an opportunity to branch the frontier of applied mechanics.

In this paper, we review a few recent theories or observations that originate from the coupling of electrochemistry and mechanics, including diffusion-induced stresses, stress-regulated surface charge transfer, interfacial reaction, inhomogeneous growth of lithiated phases, instability of solid-state reaction front (SSRF), as well as reaction-assisted plastic flow and corrosive fracture. Most of the phenomena are at the early stage of study and are to be further explored. Here, we focus on the phenomenological description using schematic illustrations without elaborating great details. It is our goal to attract interests of the community on the interdisciplinary research on mechanics and electrochemistry. Bridging the two fields with a focus of developing energy solutions can be truly far-reaching.

2 Diffusion-Induced Stresses

Diffusion of Li atoms into an electrode material is accompanied by a change of volume. This volumetric change may induce stresses if the deformation is constrained. Constraints may be geometric (e.g., a thin film electrode bonded to a substrate) or may result from an inhomogeneous distribution of Li (and hence inhomogeneous strains) within the host. The effect of

[1]Corresponding author.

Manuscript received June 11, 2016; final manuscript received November 16, 2016; published online December 12, 2016. Assoc. Editor: George Nelson.

diffusion-induced stresses in the electrode materials is now well recognized. Maybe less understood is the impact of stress on the transport of Li within the host and hence on the electrochemical potential of the cell [47]. When Li is inserted into a host, locally generated stresses due to strain mismatch modify the energy cost associated with further insertion. In other words, stress affects the chemical potential of Li in the host, whose gradient drives diffusion. The modeling of the coupling between mechanics and chemistry is thus twofold: diffusion induces stresses, and stresses affect diffusion. We sketch the stress–diffusion coupling in Fig. 1. For a free-standing spherical particle, the inhomogeneous distribution of Li induces a field of stress within the particle. For a given Li flux prescribed at the outer shell of the particle, the shell region (Li rich) is under compression and the core region (Li poor) is under tension, as shown in Fig. 1(*a*). Stress modifies the chemical potential of Li and drives migration of Li from the compressed part to the tensed core. Figure 1(*b*) sketches the comparison of radial distribution of Li in the spherical particle with and without accounting for the stress effect. Overall, the stress gradient tends to homogenize the Li distribution.

Continuum models coupling deformation to diffusion of atoms in a solid solution are certainly not new. A fundamental idea of most models is the representation of the deformation induced by insertion of guest species as an eigenstrain (stress–free strain). The analogy with thermal strain is then obvious and dates back at least to the work of Prussin [48], who analyzed stresses generated in Si wafers due to solute diffusion. Fundamental contributions to the thermodynamics of solid solutions under stresses are those of Larché and Cahn [49,50], and Li [51], who independently derived expressions for the chemical potential of diffusing species into a solid host. A comprehensive framework for diffusion coupled to large, inelastic deformations was proposed by Stephenson [52]. By contrast, analyses focusing on electrochemical insertion in electrode materials are relatively new. Relying on the analogy with thermal strains but neglecting stress effects on diffusion, early work was done to estimate the stress generated in carbon anodes [53], $LiMn_2O_4$, $LiCoO_2$ cathode, and Si anode particles [27,54–59]. The effect of stress on the activation energy for diffusion was studied by Gao et al., Cheng et al., and others [44,45,60–65]. Integrated models of the full electrochemistry of batteries were developed by Garcia et al. [66] and recently by Purkhastaya and McMeeking [67]. Diffusion-induced stresses in electrodes of different geometries have also been studied recently [68–72]. The stochastic methodology has also been adopted to study the intercalation-induced stresses and damages in electrodes by Mukherjee and coworkers [73–75]. For high-capacity electrodes, lithiation-induced strains are often accommodated by inelastic deformation. Continuum models that account for large elastoplastic deformation of the electrode have appeared more recently [42,76–81]. The simplest formula, regardless the deformation kinematics and constitutive behaviors of the electrodes, may be following [49]:

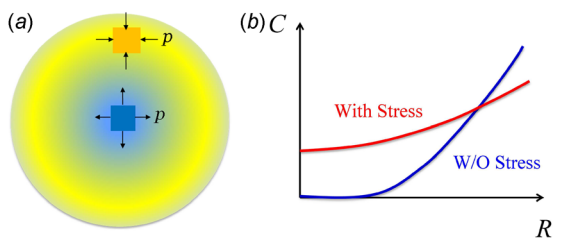

Fig. 1 (*a*) Schematic of diffusion-induced stress in a free-standing spherical particle. Li insertion causes deformation of the host material, and the inhomogeneous distribution of Li induces a field of stress within the particle. The shell region (Li rich) is under compression and the core region (Li poor) is under tension. (*b*) Sketch of the stress effect on radial distribution of Li in the spherical particle. The stress gradient tends to homogenize the Li distribution. The red line represents the Li profile calculated by considering both effects of stress and Li concentration gradient, while the blue line represents the case that Li diffusion is driven only by the concentration gradient.

$$\mu = \mu^0 + kT\log(\gamma x) - \Omega\sigma_m \tag{1}$$

which neglects the variation of the elastic constants with composition and assumes purely volumetric strain induced by lithiation. Here, μ is the chemical potential of Li in the host, μ_0 is a reference value, and x is the composition defined as the ratio of the number of Li atoms to that of the total number of atoms. The first two terms on the right-hand side of Eq. (1) are the familiar expressions of the chemical potential for a species in nonideal solution, with γ as the activity coefficients, which depends on the composition. For an ideal or dilute solution, the activity coefficient is constant. However, for insertion materials strong deviations from ideality are expected. The activity coefficient can in principle be fitted from experimental data [82,83]. The third term in Eq. (1) represents the change in elastic energy upon insertion under stress, where Ω represents the partial molar volume of Li in the host, and $\sigma_m = \sigma_{kk}/3$ is the mean stress.

3 Stress-Regulated Surface Charge Transfer

In addition to the effect on Li diffusion, mechanical stresses influence the electrical response of electrode materials [84,85]. Sethuraman et al. [84] reported that the stress affects the equilibrium potential of Si electrodes with an estimate that 1 GPa stress changes the electrical potential by ~60 mV. Piper et al. [85] found that a compressive stress leads to a higher overpotential and a lower saturation capacity at the cut-off voltage during galvanostatic operations. Stress has a similar effect of electrical overpotential and modulates the driving force of charge transfer at the electrode surface. Butler–Volmer relationship is the most common equation describing the charge transfer rate in terms of the thermodynamic driving force (i.e., overpotential). However, the stress effect is ignored in the traditional Butler–Volmer equation. Recently, researchers modified Butler–Volmer equation by incorporating the stress effect into the free energy and activation energy for the surface charge transfer process [76,86]. Figure 2 shows the free-energy diagram altered by the applied electrical potential and mechanical stresses. The activation energies of the redox reactions at equilibrium states are identical, $\Delta G_{0O} = \Delta G_{0R}$ (black-solid lines). The chemical equilibrium will be broken by the electrical overpotential $E - E_0$ as well as the mechanical stress, where E represents the electrical field and E_0 the equilibrium potential. The electrical overpotential promotes electron transfer and decreases the free energy of the oxidized state by $F(E - E_0)$ (red-dashed line). The tensile stress in the surface layer, on the other hand, causes a change of elastic energy $\Delta W = \sigma_m\Omega$ (blue-dashed line) that promotes the formation of neutral Li. The change in the total free energy of the reduced state relative to the oxidized state is $F(E - E_0) - \sigma_m\Omega$. By introducing the charge transfer coefficient α, the stress effect is included in the Butler–Volmer equation in the following form [86]:

$$i = i_0\left\{\exp\left[(1-\alpha)\frac{F(E-E_0)-\sigma_m\Omega}{RT}\right] - \exp\left[\alpha\frac{F(E-E_0)-\sigma_m\Omega}{RT}\right]\right\} \tag{2}$$

where i_0 is the exchange current density, R is the universal gas constant, T is the temperature, and F is the Faraday constant. The modified Butler–Volmer equation indicates that tensile stresses would facilitate the combination of Li ions and electrons and thus lithiation reactions.

In a recent report, Kim et al. [87] made an ingenious use of the principle of stress-driven diffusion to design a novel class of mechanical energy harvesters. The experimental setup is

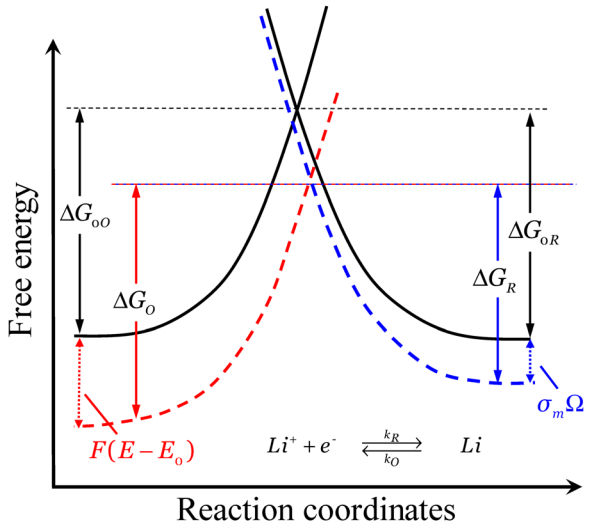

Fig. 2 Free-energy diagram for the surface charge transfer process altered by the applied electrical potential and mechanical stresses. The activation energies of the redox reactions at equilibrium states are identical, $\Delta G_{0O} = \Delta G_{0R}$ (black-solid lines). The chemical equilibrium will be broken by the electrical overpotential as well as mechanical stress. The electrical overpotential $E - E_0$ promotes electron transfer and decreases the free energy of the oxidized state by $F(E - E_0)$ (red-dashed line). The tensile stress in the surface layer causes a change of elastic energy $\Delta W = \sigma_m\Omega$ (blue-dashed line) and promotes the formation of neutral Li atoms. The change in the total free energy of the reduced state relative to the oxidized state is $F(E - E_0) - \sigma_m\Omega$.

schematically shown in Fig. 3(*a*). Two identical partially lithiated Si films serve as electrodes separated by electrolyte-soaked polymer membranes. Bending-induced asymmetric stresses generate chemical potential difference, driving migration of Li ions from the compressed electrode (red) to the tensed side (blue) to generate electrical current. By removing the bending stress, ion flux and electrical concurrent are reversed. The device can sustain more than a thousand cycles with nearly constant current output. Furthermore, the device exhibits higher average energy output than most piezoelectric generators when operating at low frequencies. In this design, the electrical current density depends on the magnitude of bending-induced asymmetric stresses. The characteristic of the output electric current is determined by the concurrent surface charge transfer and Li bulk diffusion in the electrodes—both

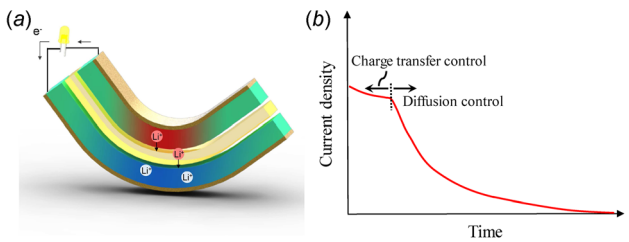

Fig. 3 (*a*) Design of mechanical energy harvester based on the stress-driven Li diffusion. Two identical partially lithiated Si films act as electrodes, separated by electrolyte-soaked polymer membranes (the size of the electrodes and electrolyte is not in scale). Bending-induced asymmetric stresses generate chemical potential difference, driving migration of Li ions from the compressed electrode (red) to the tensed side (blue). (*b*) Schematic of short circuit current density during the release of bending. The peak current is determined by the Butler–Volmer surface charge transfer process, and the subsequent state is controlled by Li diffusion in the electrodes. (Figure 3(*a*) is reproduced with permission from Kim et al. [87]. Copyright 2015 by the Nature Publishing Group.)

processes are dependent on the bending stresses. Figure 3(*b*) shows the schematic of the current density upon release of bending (quantitative results are to be published in a separate work). At the short-range time scale, the peak of output current is limited by the Butler–Volmer surface charge transfer process. In the following stage, the bulk transport of Li through the electrodes becomes the rate-limiting step. The current density eventually diminishes to zero until new equilibrium state is reached. By examining the experimental measurement of the current density, we are able to identify the surface charge transfer controlled or diffusion-controlled regime. This feature also enables one to control the current density of mechanical energy harvesters through manipulating the geometry of the electrodes in order to optimize the energy efficiency of the device. The work by Kim et al. is a clear demonstration of interactions between stresses and electrochemistry and opens the avenues of optimizing electrochemical devices for mechanical sensing and actuation.

4 Stress-Regulated Interfacial Reaction

The operation of an electrochemical cell involves a number of kinetic processes, including Li diffusion through the electrodes and the electrolyte, electron transport, redox reactions at the interface, lithiation at the reaction front, and phase transition of the electrode materials. Lithiation reaction involves short-range processes, such as breaking and forming of atomic bonds. It is now evident that lithiation of some systems results in interfacial reaction-controlled kinetics. For instance, initial lithiation of crystalline Si generates an atomically sharp planar interface separating crystalline Si from amorphous-lithiated Si and the deformation is highly anisotropic [88–90]. Meanwhile, to accommodate the large volumetric expansion associated with the lithiation process, the host material must deform plastically. By considering the interfacial reaction and the elastoplastic deformation, we have constructed a theory that accounts for concurrent reaction kinetics and plasticity that allows us to explore the stress-regulated interfacial reactions, inhomogeneous growth of lithiated phase, as well as the instability of solid-state reaction front. In Secs. 4.1 to 4.3, we will briefly introduce the respective theories and quote experimental observations that verify those ideas.

4.1 Stagnation of Reaction Front Propagation. The most dramatic effect of stress on electrochemical reactions may be the stress-induced stagnation of reaction front during lithiation of Si spherical particles. To establish a theoretical basis, we identify the driving force for the reaction—the change in the free energy associated with the reaction that converts one Li atom and $1/x$ number of Si atoms into lithiated Si [29]. Let ΔG_r be the free energy when both the stress and the applied voltage vanish. When the conducting wire is connected through a voltage source, associated with converting one Li atom into lithiated Si, one electron passes through the conducting wire, so that the external voltage source does work $e\Phi$, where Φ is the voltage, and e is the elementary charge. The driving force is modified when the two phases, the crystalline Si and the lithiated Si, are stressed. Associated with converting one Li atom into lithiated Si, the crystalline Si phase loses $1/x$ number of Si atoms, and the stress in silicon does work $-\sigma_m^{\mathrm{Si}}\Omega^{\mathrm{Si}}/x$, where σ_m^{Si} is the mean stress in Si at the reaction front, and Ω^{Si} is the volume per Si atom. The amorphous phase gains $1/x$ number of Si atoms and one Li atom, so that the stress in the amorphous phase does work $\sigma_m^{\mathrm{Li}_x\mathrm{Si}}\Omega^{\mathrm{Li}_x\mathrm{Si}}/x$, where $\sigma_m^{\mathrm{Li}_x\mathrm{Si}}$ is the mean stress in the amorphous phase at the reaction front, and $\Omega^{\mathrm{Li}_x\mathrm{Si}}$ is the volume per unit of $\mathrm{Li}_x\mathrm{Si}$. Combining the above contributions, we find that, when the reaction advances, the net change in the free energy is [29]

$$\Delta G = \Delta G_r - e\Phi + \frac{1}{x}\left(\sigma_m^{\mathrm{Si}}\Omega^{\mathrm{Si}} - \sigma_m^{\mathrm{Li}_x\mathrm{Si}}\Omega^{\mathrm{Li}_x\mathrm{Si}}\right) \tag{3}$$

We have neglected the dissipation at electrolyte/electrode interfaces as well as inside the electrodes and electrolytes. In our sign

convention, a negative ΔG drives lithiation, and a more negative value represents a larger driving force. The free energy of reaction ΔG_r takes a negative value. We also take the polarity of the voltage source in the direction that drives lithiation. As expected, a compressive mean stress in the crystalline Si promotes lithiation, but a compressive mean stress in the lithiated Si retards lithiation.

We can derive the stress field in a spherical Si particle [29] and examine how the stress field modifies the driving force for the lithiation reaction. The free energy contributed by stresses is plotted in Fig. 4(*a*). The horizontal axis represents the normalized radius of the crystalline core, where a represents the radius of the crystalline Si core, and b the outer radius of the Si particle. As expected, the contribution due to the stresses is positive and retards lithiation. The magnitude of the contribution increases as the crystalline core shrinks. Recall that the free energy of formation of lithiated silicon is small; for example, $\Delta G_r = -0.18$ eV for amorphous $Li_{2.1}Si$ [91]. Consequently, the reaction can readily generate large enough stress to counteract the electrochemical driving force, stalling the reaction. Such a stagnation effect was observed in a recent experimental study of the kinetics of crystalline Si particle lithiation with in situ transmission electron microscopy (TEM). McDowell et al. monitored the propagation of the lithiation reaction front described by the ratio a/b, see Fig. 4(*b*) [92]. This figure shows that the propagation of the reaction front is significantly slowed at similar ratios of a/b for particles with different sizes, which suggests that the large compressive stress built up as the ratio a/b decreases retards the lithiation reaction.

4.2 Inhomogeneous Growth of Lithiated Phase. For the system with interfacial reaction controlled kinetics, the stress field will be modified by the geometric factor of surface curvature [93]. When the reaction front is flat (e.g., thin film case), the volumetric expansion associated with the reaction is accommodated by elongating the lithiated phase in the direction normal to the reaction front, while maintaining the geometric compatibility between the two phases in the directions tangential to the reaction front. As the reaction front advances, previously lithiated material recedes by rigid-body translation with no further deformation. The stresses in the lithiated phase remain compressive state. When the reaction front is convex (e.g., lithiation on the surface of nanowires and spherical particles), the lithiated phase recedes as the reaction front advances. An element of lithiated material at the front initially undergoes compressive stress in the hoop directions. While upon subsequent lithiation, the element is pushed away and then develops a tensile stress in the hoop directions. The tensile stress may increase the solubility of Li and facilitate Li transport through the lithiated material. On the contrary, when the reaction front is concave (e.g., lithiation on the inner face of the nanotubes), the stress field is reversed and the lithiated phase is subjected to compressive stresses. For a system with alternative convex and concave surface curvatures (Fig. 5(*a*)), the lithiated phase may grow to a wavy morphology because of the asymmetric field of stresses. In a recent study, we [93] used in situ TEM to observe the lithiation behavior of SiO_2 coating on SiC nanowires. SiC is inert to Li reaction so the entire deformation is due to the lithiation of SiO_2 thin coating. Figure 5(*b*) shows the inhomogeneous growth of SiO_2 during the cycle of lithiation and delithiation. It forms a wavy structure that parts of the surface grow thicker than others. In a high-resolution TEM image (details in Ref. [93]), the pristine SiO_2@SiC nanowire has a twinning microstructure that induces alternative convex and concave curvatures. It is plausible that the tensile stress field associated with the convex surface grows a thicker layer of the lithiated phase. Such a stress-mediated growth shows an interesting mechanism of nonuniform morphology and may also provide an alternative way to fabricate complex patterned nanostructures in other electromechanical systems [94,95].

4.3 Instability of Solid-State Reaction Front. Another interesting phenomenon that we recently observed is the instability of solid-state reaction front modulated by mechanical stresses. In an example study of ZnO nanowire, lithiation-induced stress breaks the planar solid-state reaction front into a curved interface and results in an uneven lithiation on a given basal plane [96]. Figure 6(*a*) sketches the lithiation behavior of a single ZnO nanowire. Once a reliable contact is made between the nanowire with the counter electrode and the electrolyte Li/Li_2O, Li ions diffuse quickly on the nanowire surface, forming a thin wetting layer with typical thickness of a few nanometers. The nanowire is first lithiated radially and the extent of lithiation is limited by the amount of Li transport through the thin wetting layer. The solid-state reaction front primarily propagates along the longitudinal direction of the nanowire away from the electrolyte. The radial lithiation forms a structure of lithiated shell and unlithiated core. A field of stress is associated with the core-shell geometry. While the tensile stress in the lithiated shell induces discrete surface cracks and facilitates Li transport through the crack surfaces, the compressive stress in the pristine core diminishes the thermodynamic driving force of the electrochemical reaction and impedes the local lithiation. The asymmetry of the characteristic stresses breaks the

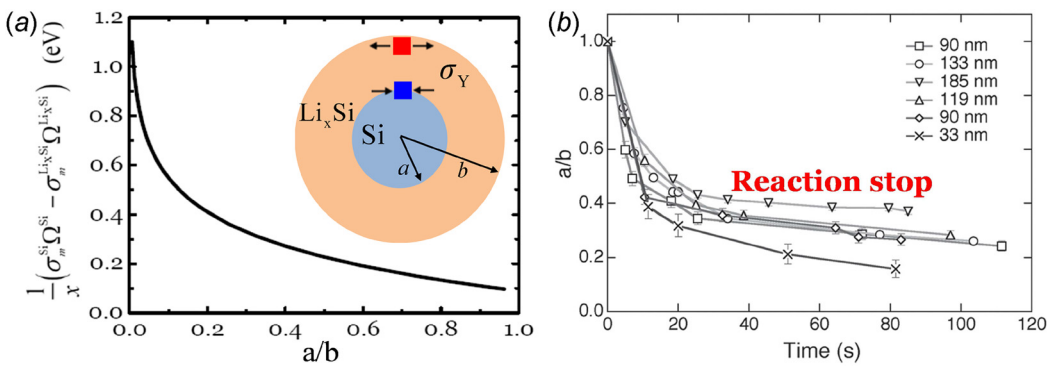

Fig. 4 (*a*) Stress-regulated interfacial reaction during lithiation of a crystalline Si spherical particle. Stress modifies the free energy associated with the reaction that converts one Li and 1/*x* Si atoms into lithiated Si at the reaction front. The figure plots the evolution of the free energy contributed by mechanical stresses as a function of the position of the reaction front. The inset shows the schematic of the stress field within the particle (Reproduced with permission from Zhao et al. [29]. Copyright 2012 by the Electrochemical Society). (*b*) Experimental evidence of the stagnation of lithiation reaction due to the stress effect. Lithiation in the particles of different sizes significantly slows down at similar *a*/*b* ratios suggesting that stress gradually builds up as the *a*/*b* ratio decreases and retards the progression of the reaction front (Reproduced with permission from McDowell et al. [92]. Copyright 2012 by John Wiley and Sons).

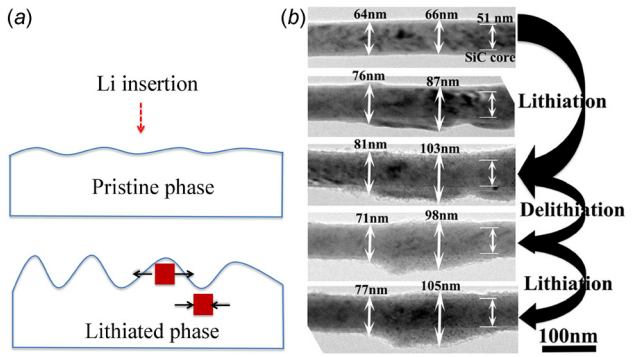

Fig. 5 (*a*) Schematic of inhomogeneous growth of lithiated phase due to the stress-regulated lithiation reaction. The lithiated phase of convex curvature develops a field of tensile stresses, facilitating Li transport through the lithiated material and promoting the interfacial reaction at the phase boundary. On the contrary, the lithiated phase of concave curvature is under a field of compressive stresses, retarding the electrochemical growth of the layer. (*b*) In situ TEM observation of the inhomogeneous growth of the SiO_2 layer during the cycle of lithiation and delithiation. (Reproduced with permission from Zhang et al. [93]. Copyright 2014 by the American Chemical Society).

planar SSRF into a curved interface that is a reminiscence of Mullins–Sekerka interfacial instability during solidification of liquids. Figure 6(*b*) shows the in situ TEM observation of time evolution of the curved SSRF. The magnitude of compressive stresses increases toward the core, dictating a gradually decreasing driving force of lithiation from the surface to the center of the nanowire. The pattern of the reaction front shown in Fig. 6(*b*) corroborates the transition of the stress state. The radius of curvature gradually decreases and the core is eventually lithiated as the reaction front propagates.

5 Reactive Flow of Materials

When considering the coupled diffusion and plastic deformation, most theories have assumed that, in each small element of the host, the reaction (or insertion) has reached equilibrium, while plastic flow is a nonequilibrium process. The local effects of Li insertion are limited to the induced deformation and the change in mechanical properties [97–99]. This physical picture has been adopted despite the observation that both reaction and flow are mediated by breaking and reforming atomic bonds. In the continuum theory, this assumption precludes a powerful coupling between reaction and flow: when local chemical equilibrium has not been reached, the driving force for the reaction can result in breaking and forming atomic bonds, enabling plastic flow under lower deviatoric stress. The plastic flow assisted by the chemical reaction is so-called reactive flow [33]. Figure 7(*a*) sketches the atomistic picture of a material under concurrent electrochemical reaction and mechanical load. When the host material is subject to lithiation, the insertion of Li atoms constantly breaks the atom bonds of the host material and results in a dynamic change of valence state of matter. Figure 7(*b*) shows that the stress needed to maintain a given shear displacement with concurrent chemical reaction should be lower than that needed for pure mechanical load. Through ab initio calculations and in situ experimental measurement, we found that the magnitude of yield strength under mechanical load alone is about twice as high as that during lithiation reaction [33].

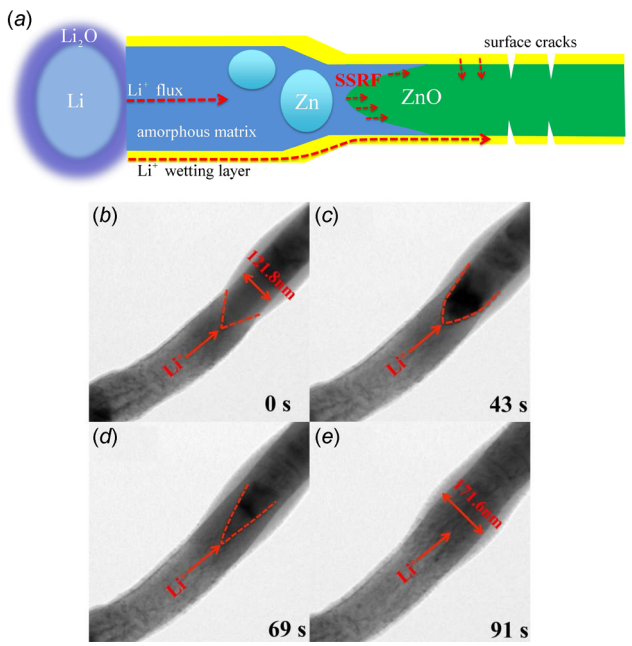

Fig. 6 (*a*) Stress-induced instability of solid-state reaction front (SSRF) during lithiation of the ZnO nanowires. Li ions diffuse quickly on the nanowire surface, forming a thin wetting layer with typical thickness of a few nanometers. The primary SSRF propagates along the longitudinal direction of the nanowire away from the electrolyte. Lithiation induces a field of tensile stress in the lithiated shell, and compressive stress in the unlithiated core. The stress field regulates the lithiation reaction and breaks the planar SSRF into a curved interface. (*b*)–(*e*) In situ TEM observation on the evolution of the curved reaction front. The radius of curvature gradually decreases, and the core is eventually lithiated as the reaction front propagates (Reproduced with permission from Zhang et al. [96]. Copyright 2015 by Elsevier).

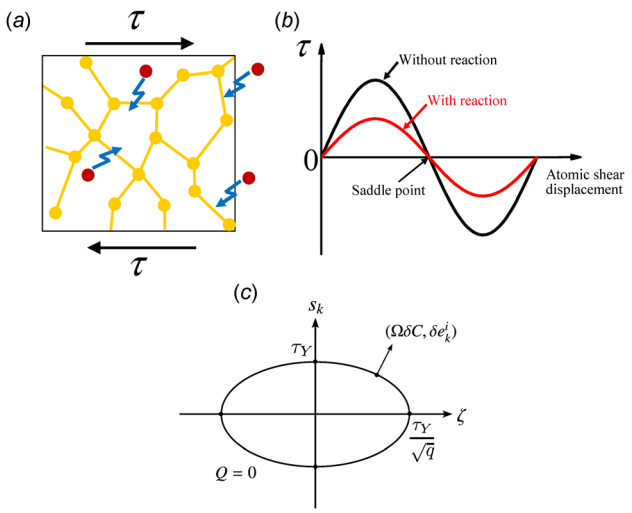

Fig. 7 (*a*) Schematic illustration of concurrent Li insertion and plastic deformation. The host atom bonds are broken by the insertion of Li, and the valence state of matter is under dynamic change. (*b*) The stress needed to maintain a given shear displacement with ongoing chemical reaction is lower than that needed for pure mechanical load. (*c*) A yield function $Q(s_1,s_2,s_3,\zeta)$ is sketched in the space of (s_k,ζ); the condition $Q = 0$ defines the yield. (δe^i_k, $\Omega\delta C$) represents the increment of inelastic deformation driven by both the mechanical load s_k and the chemomechanical load ζ. Under pure shear loading, plastic flow occurs when the shear stress s_k reaches the yield strength τ_Y. Under the condition of insertion without stress, inelastic volume change occurs when the chemomechanical load ζ reaches $\tau_Y/\sqrt{q}$.

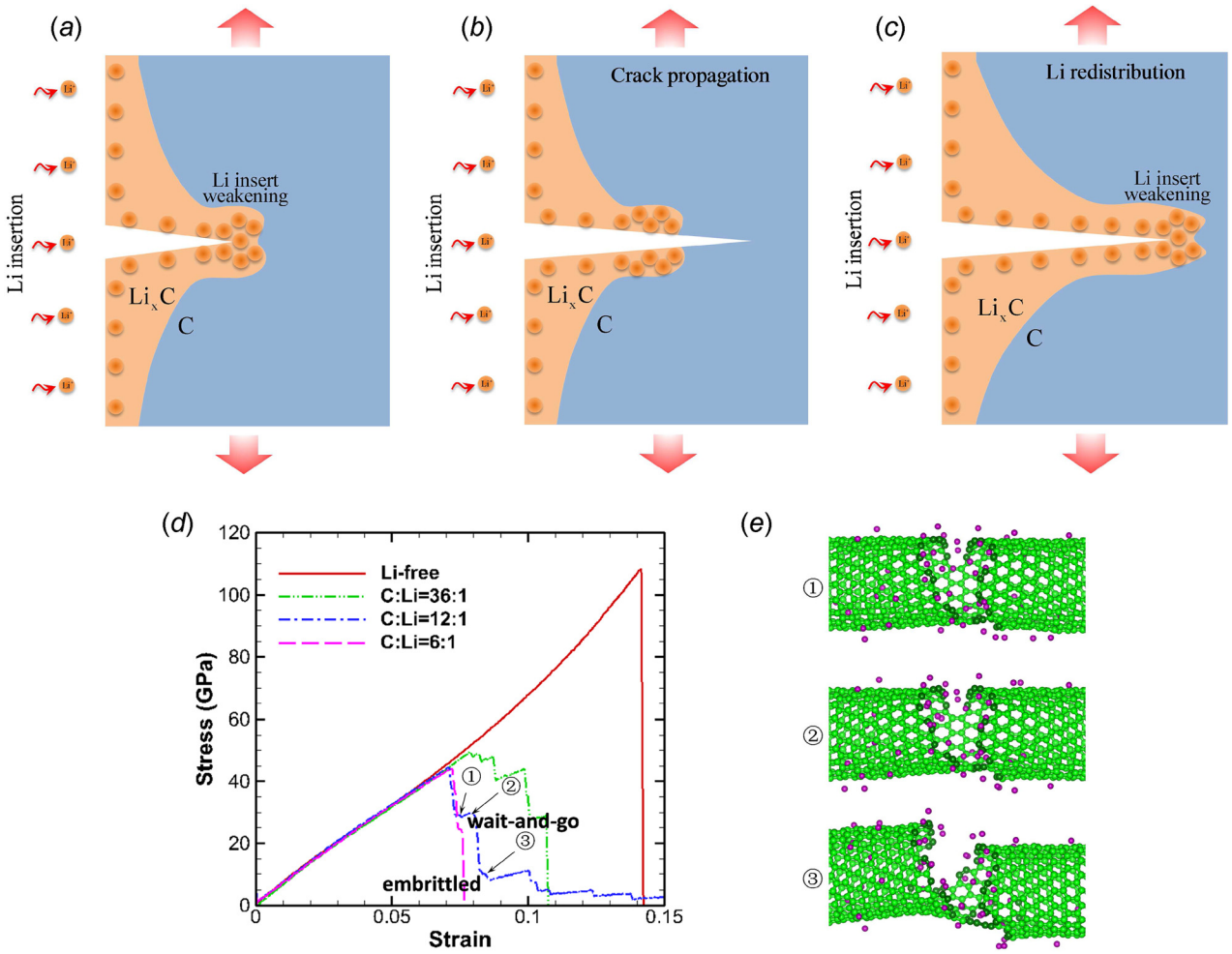

Fig. 8 (*a*)–(*c*) Schematic of the wait-and-go fracture behavior induced by the concurrent Li diffusion, Li weakening at the crack tip, and crack propagation. (*d*) Stress–strain curves of the SWCNTs containing a holelike defect. (*e*) Three stages of SWCNTs showing the corrosive fracture behavior of SWCNTs studied by molecular dynamics simulations (Reproduced with permission from Huang et al. [35]. Copyright 2013 by AIP Publishing LLC).

We proposed a theory to treat both insertion and flow as nonequilibrium processes and place the driving forces for flow and reaction on equal footing. This theory is able to predict flow under combined chemomechanical loading for a host too brittle to flow under mechanical load alone. We defined a chemomechanical load ζ that drives the Li insertion, and the deviatoric stresses $s_k = \sigma_k - \sigma_m$ that drives the plastic flow. We generalize von Mises theory of plasticity to include the chemomechanical loading. We introduce the following yield function $Q = Q(s_1, s_2, s_3, \zeta)$ [33,34]:

$$Q = \frac{1}{2}\left(s_1^2 + s_2^2 + s_3^2\right) + q\zeta^2 - \tau_Y^2 \tag{4}$$

where q indicates the relative contributions of the mechanical and chemical driving forces. The condition $Q = 0$ defines the yield surface in the driving forces space. The yield surface is shown schematically in Fig. 7(*c*). The yield strength τ_Y is determined when the host is subject to pure shear loading condition in the absence of chemical driving force. Under the condition of insertion without stress, the yield condition on the driving force for reaction is $\zeta = \zeta_Y \equiv \tau_Y/\sqrt{q}$. Under combined chemomechanical load, the shear stress needed for flow will be lower than the yield stress under pure mechanical load. Adopting the normality postulate, a flow rule for each flux variable is obtained by differentiating the yield function with respect to the corresponding driving force. For a rate-independent model, it yields [34]

$$\delta e_k^i = \alpha\frac{\partial Q}{\partial s_k}, \quad \Omega\delta C = \alpha\frac{\partial Q}{\partial \zeta} \tag{5}$$

During yielding, the plastic multiplier α is determined by requiring the set of driving forces to remain on the yield surface. It is noteworthy that the coupling of chemical reactions and plasticity has also been studied by recent theories of anisotropic compositional expansion [100–102] and glassy relaxation [103].

6 Corrosive Fracture of Electrodes

Fracture and fatigue occur in most of the electrode materials, and numerous models have been developed to analyze fracture in Li-ion batteries. Different approaches were adopted in literature [29,53,73,104–107]. Several groups incorporated diffusion-induced stress calculations and used a stress criterion to predict the onset of fracture [19,45,53,107]. Another set of literature have studied lithiation-induced fracture by applying Griffith fracture mechanics [29,105,106]. Recent studies employed Paris' Law in combination with chemical degradation to predict the cyclic fatigue [108]. To date, few studies have looked into the concurrent Li transport and crack propagation. Li is like a corrosive species. Li insertion breaks the host atomic bonds and forms weaker bonds between Li and host atoms, decreasing both elastic modulus and fracture strength of the host material [109–114]. The dynamics of crack propagation should be coupled with the redistribution of Li.

In particular, Li diffuses quickly on the crack surface because of the high surface diffusivity and is accumulated at the crack tip due to the large tensile stresses ahead of the crack. In a recent work, it is found that local tensile stress field around the crack tip decreases the chemical potential and attracts Li accumulation at the crack tip [115]. As a result, aggregated Li reduces the fracture toughness of the host material, acting as a corrosive agent that accelerates crack nucleation and propagation [116]. This phenomenon is a reminiscence of corrosive fracture of metals induced by oxygen or moisture at the crack tip. However, different from oxygen, Li might be a more corrosive species because the formation of oxides at the crack tip may shield further oxygen transport and protect unstable crack propagation [117–119], while lithiated alloys do not usually have such an effect.

Huang et al. [35] recently investigated lithiation-mediated corrosive failure in defective single-walled carbon nanotubes (SWCNTs) using molecular dynamics simulations. They found that the coupling between fracture and Li diffusion would cause two distinct fracture modes: abrupt and retarded fracture. Abrupt fracture involves spontaneous Li weakening of the propagating crack tip, while retarded fracture features a "wait-and-go" crack extension process in which the crack tip periodically arrests and waits to be weakened by diffusing Li before extension resumes [35]. Figures 8(*a*)–8(*c*) sketch the wait and go behavior. Initially, the crack maintains a steady state under a given external tension load. When lithiation proceeds, Li ions accumulate around the crack tip, weakening the fracture strength of the material around the crack tip, see Fig. 8(*a*). If fracture strength drops to be lower than the energy release rate, crack starts propagating which creates fresh surfaces without Li, see Fig. 8(*b*). Without the participation of Li at the crack tip, fracture strength of the material recovers and the crack will stop and wait to be weakened again by Li diffusion before the propagation resumes, see Fig. 8(*c*). Depending on the times scales of Li diffusion and crack propagation, Li may always catch up the crack propagation when it extends, inducing an abrupt fracture of the electrodes. Figure 8(*d*) shows stress–strain curves of SWCNTs containing a holelike defect. Figure 8(*e*) provides three fractural states of SWCNTs that show the corrosive fracture behavior of SWCNTs based on molecular dynamics simulations. More recently, Klinsmann et al. [120] studied fracture–diffusion coupling using a phase-field approach. Similar abrupt and wait-and-go fracture behaviors were reported in their model.

7 Conclusions

Mechanical issues are universal in all forms of energy conversion, storage, and harvesting. Here, we review recent progress on the intimate relationship between mechanics and electrochemistry in an example system of Li-ion batteries. The electrochemical processes of Li insertion and extraction in the electrodes induce a wealth of phenomena of elemental ingredients of mechanics. Meanwhile, mechanical stresses place nontrivial effects on the thermodynamics and kinetics of electrochemical reactions, such as stress-modulated ion diffusion, surface charge transfer, stagnation and instability of solid-state reaction front, as well as lithiation-assisted plasticity and fracture of electrodes. This paper focuses on the schematic illustration of the basic ideas rather than elaborate great details behind each theory. It is our hope to attract further interests of the community on the emerging field of electrochemomechanics in the application of energy materials. The fundamental understanding of the intimate coupling between mechanics and electrochemistry may provide an opportunity to advance the frontier of mechanics as well as create knowledge significant to the technologies of high-performance batteries.

Acknowledgment

This work was supported by the National Science Foundation through the Grant No. CBET-1603866. K.Z. is also grateful for the support of 3M nontenured faculty award.

Reference

[1] Armand, M., and Tarascon, J. M., 2008, "Building Better Batteries," Nature, **451**(7179), pp. 652–657.
[2] Whittingham, M. S., 2008, "Materials Challenges Facing Electrical Energy Storage," MRS Bull., **33**(4), pp. 411–419.
[3] Scrosati, B., and Garche, J., 2010, "Lithium Batteries: Status, Prospects and Future," J. Power Sources, **195**(9), pp. 2419–2430.
[4] Nitta, N., Wu, F., Lee, J. T., and Yushin, G., 2015, "Li-Ion Battery Materials: Present and Future," Mater. Today, **18**(5), pp. 252–264.
[5] Kasavajjula, U., Wang, C., and Appleby, A. J., 2007, "Nano- and Bulk-Silicon-Based Insertion Anodes for Lithium-Ion Secondary Cells," J. Power Sources, **163**(2), pp. 1003–1039.
[6] Zhang, W. J., 2011, "A Review of the Electrochemical Performance of Alloy Anodes for Lithium-Ion Batteries," J. Power Sources, **196**(1), pp. 13–24.
[7] McDowell, M. T., Xia, S., and Zhu, T., 2016, "The Mechanics of Large-Volume-Change Transformations in High-Capacity Battery Materials," Extreme Mech. Lett., **9**(Pt. 3), pp. 480–494.
[8] Cannarella, J., and Arnold, C. B., 2014, "Stress Evolution and Capacity Fade in Constrained Lithium-Ion Pouch Cells," J. Power Sources, **245**, pp. 745–751.
[9] Sun, H., Xin, G., Hu, T., Yu, M., Shao, D., Sun, X., and Lian, J., 2014, "High-Rate Lithiation-Induced Reactivation of Mesoporous Hollow Spheres for Long-Lived Lithium-Ion Batteries," Nat. Commun., **5**, p. 4526.
[10] Baggetto, L., Danilov, D., and Notten, P. H. L., 2011, "Honeycomb-Structured Silicon: Remarkable Morphological Changes Induced by Electrochemical (De)Lithiation," Adv. Mater., **23**(13), pp. 1563–1566.
[11] Chan, C. K., Peng, H., Liu, G., McIlwrath, K., Zhang, X. F., Huggins, R. A., and Cui, Y., 2008, "High-Performance Lithium Battery Anodes Using Silicon Nanowires," Nat. Nanotechnol., **3**(1), pp. 31–35.
[12] Kim, H., Han, B., Choo, J., and Cho, J., 2008, "Three-Dimensional Porous Silicon Particles for Use in High-Performance Li Secondary Batteries," Angew. Chem., **120**(52), pp. 10305–10308.
[13] Liu, N., Wu, H., McDowell, M. T., Yao, Y., Wang, C. M., and Cui, Y., 2012, "A Yolk-Shell Design for Stabilized and Scalable Li-Ion Battery Alloy Anodes," Nano Lett., **12**(6), pp. 3315–3321.
[14] Wu, H., Zheng, G. Y., Liu, N. A., Carney, T. J., Yang, Y., and Cui, Y., 2012, "Engineering Empty Space Between Si Nanoparticles for Li-Ion Battery Anodes," Nano Lett., **12**(2), pp. 904–909.
[15] Yao, Y., McDowell, M. T., Ryu, I., Wu, H., Liu, N., Hu, L., Nix, W. D., and Cui, Y., 2011, "Interconnected Silicon Hollow Nanospheres for Lithium-Ion Battery Anodes With Long Cycle Life," Nano Lett., **11**(7), pp. 2949–2954.
[16] Cui, L. F., Hu, L. B., Choi, J. W., and Cui, Y., 2010, "Light-Weight Free-Standing Carbon Nanotube-Silicon Films for Anodes of Li-Ion Batteries," ACS Nano, **4**(7), pp. 3671–3678.
[17] Wang, C. M., Li, X. L., Wang, Z. G., Xu, W., Liu, J., Gao, F., Kovarik, L., Zhang, J. G., Howe, J., Burton, D. J., Liu, Z. Y., Xiao, X. C., Thevuthasan, S., and Baer, D. R., 2012, "In Situ TEM Investigation of Congruent Phase Transition and Structural Evolution of Nanostructured Silicon/Carbon Anode for Li Ion Batteries," Nano Lett., **12**(3), pp. 1624–1632.
[18] Yamada, M., Ueda, A., Matsumoto, K., and Ohzuku, T., 2011, "Silicon-Based Negative Electrode for High-Capacity Li-Ion Batteries: "SiO"-Carbon Composite," J. Electrochem. Soc., **158**(4), pp. A417–A421.
[19] Sandu, G., Brassart, L., Gohy, J. F., Pardoen, T., Melinte, S., and Vlad, A., 2014, "Surface Coating Mediated Swelling and Fracture of Silicon Nanowires During Lithiation," ACS Nano, **8**(9), pp. 9427–9436.
[20] Wang, J. W., Liu, X. H., Zhao, K. J., Palmer, A., Patten, E., Burton, D., Mao, S. X., Suo, Z. G., and Huang, J. Y., 2012, "Sandwich-Lithiation and Longitudinal Crack in Amorphous Silicon Coated on Carbon Nanofibers," ACS Nano, **6**(10), pp. 9158–9167.
[21] Nowack, L. V., Bunjaku, T., Wegner, K., Pratsinis, S. E., Luisier, M., and Wood, V., 2015, "Design and Fabrication of Microspheres With Hierarchical Internal Structure for Tuning Battery Performance," Adv. Sci., **2**(6), p. 1500078.
[22] Magasinski, A., Dixon, P., Hertzberg, B., Kvit, A., Ayala, J., and Yushin, G., 2010, "High-Performance Li-Ion Nodes Using a Hierarchical Bottom-Up Approach," Nat. Mater., **9**(4), pp. 353–358.
[23] Chen, X. L., Gerasopoulos, K., Guo, J. C., Brown, A., Wang, C. S., Ghodssi, R., and Culver, J. N., 2011, "A Patterned 3D Silicon Anode Fabricated by Electrodeposition on a Virus-Structured Current Collector," Adv. Funct. Mater., **21**(2), pp. 380–387.
[24] Haftbaradaran, H., Xiao, X. C., Verbrugge, M. W., and Gao, H. J., 2012, "Method to Deduce the Critical Size for Interfacial Delamination of Patterned Electrode Structures and Application to Lithiation of Thin-Film Silicon Islands," J. Power Sources, **206**, pp. 357–366.
[25] Soni, S. K., Sheldon, B. W., Xiao, X. C., Verbrugge, M. W., Ahn, D., Haftbaradaran, H., and Gao, H. J., 2012, "Stress Mitigation During the Lithiation of Patterned Amorphous Si Islands," J. Electrochem. Soc., **159**(1), pp. A38–A43.
[26] Beaulieu, L. Y., Eberman, K. W., Turner, R. L., Krause, L. J., and Dahn, J. R., 2001, "Colossal Reversible Volume Changes in Lithium Alloys," Solid State Lett., **4**(9), pp. A137–A140.
[27] Zhao, K., Pharr, M., Vlassak, J. J., and Suo, Z., 2010, "Fracture of Electrodes in Lithium-Ion Batteries Caused by Fast Charging," J. Appl. Phys., **108**(7), p. 073517.
[28] Mukhopadhyay, A., and Sheldon, B. W., 2014, "Deformation and Stress in Electrode Materials for Li-Ion Batteries," Prog. Mater. Sci., **63**, pp. 58–116.

[29] Zhao, K., Pharr, M., Wan, Q., Wang, W. L., Kaxiras, E., Vlassak, J. J., and Suo, Z., 2012, "Concurrent Reaction and Plasticity During Initial Lithiation of Crystalline Silicon in Lithium-Ion Batteries," J. Electrochem. Soc., **159**(3), pp. A238–A243.
[30] Choi, J. W., McDonough, J., Jeong, S., Yoo, J. S., Chan, C. K., and Cui, Y., 2010, "Stepwise Nanopore Evolution in One-Dimensional Nanostructures," Nano Lett., **10**(4), pp. 1409–1413.
[31] Liu, X. H., Huang, S., Picraux, S. T., Li, J., Zhu, T., and Huang, J. Y., 2011, "Reversible Nanopore Formation in Ge Nanowires During Lithiation–Delithiation Cycling: An In Situ Transmission Electron Microscopy Study," Nano Lett., **11**(9), pp. 3991–3997.
[32] Zhao, K., Wang, W. L., Gregoire, J., Pharr, M., Suo, Z., Vlassak, J. J., and Kaxiras, E., 2011, "Lithium-Assisted Plastic Deformation of Silicon Electrodes in Lithium-Ion Batteries: A First-Principles Theoretical Study," Nano Lett., **11**(7), pp. 2962–2967.
[33] Zhao, K., Tritsaris, G. A., Pharr, M., Wang, W. L., Okeke, O., Suo, Z., Vlassak, J. J., and Kaxiras, E., 2012, "Reactive Flow in Silicon Electrodes Assisted by the Insertion of Lithium," Nano Lett., **12**(8), pp. 4397–4403.
[34] Brassart, L., and Suo, Z., 2013, "Reactive Flow in Solids," J. Mech. Phys. Solids, **61**(1), pp. 61–77.
[35] Huang, X., Yang, H., Liang, W., Raju, M., Terrones, M., Crespi, V. H., van Duin, A. C., and Zhang, S., 2013, "Lithiation Induced Corrosive Fracture in Defective Carbon Nanotubes," Appl. Phys. Lett., **103**(15), p. 153901.
[36] Xu, R., Vasconcelos, L. S., and Zhao, K., 2016, "Computational Analysis of Chemomechanical Behaviors of Composite Electrodes in Li-Ion Batteries," J. Mater. Res., **31**(18), pp. 2715–2727.
[37] Yang, H., Liang, W., Guo, X., Wang, C. M., and Zhang, S., 2015, "Strong Kinetics-Stress Coupling in Lithiation of Si and Ge Anodes," Extreme Mech. Lett., **2**, pp. 1–6.
[38] Sheldon, B. W., Soni, S. K., Xiao, X., and Qi, Y., 2011, "Stress Contributions to Solution Thermodynamics in Li-Si Alloys," Electrochem. Solid-State Lett., **15**(1), pp. A9–A11.
[39] Sethuraman, V. A., Chon, M. J., Shimshak, M., Srinivasan, V., and Guduru, P. R., 2010, "In Situ Measurements of Stress Evolution in Silicon Thin Films During Electrochemical Lithiation and Delithiation," J. Power Sources, **195**(15), pp. 5062–5066.
[40] Pharr, M., Suo, Z., and Vlassak, J. J., 2014, "Variation of Stress With Charging Rate Due to Strain-Rate Sensitivity of Silicon Electrodes of Li-Ion Batteries," J. Power Sources, **270**, pp. 569–575.
[41] Spaepen, F., 2005, "A Survey of Energies in Materials Science," Philos. Mag., **85**(26), pp. 2979–2987.
[42] Zhao, K., Pharr, M., Cai, S., Vlassak, J. J., and Suo, Z., 2011, "Large Plastic Deformation in High-Capacity Lithium-Ion Batteries Caused by Charge and Discharge," J. Am. Ceram. Soc., **94**(s1), pp. s226–s235.
[43] Soni, S. K., Sheldon, B. W., Xiao, X., Bower, A. F., and Verbrugge, M. W., 2012, "Diffusion Mediated Lithiation Stresses in Si Thin Film Electrodes," J. Electrochem. Soc., **159**(9), pp. A1520–A1527.
[44] Gao, Y. F., and Zhou, M., 2011, "Strong Stress-Enhanced Diffusion in Amorphous Lithium Alloy Nanowire Electrodes," J. Appl. Phys., **109**(1), p. 014310.
[45] Gao, Y. F., and Zhou, M., 2013, "Coupled Mechano-Diffusional Driving Forces for Fracture in Electrode Materials," J. Power Sources, **230**, pp. 176–193.
[46] Pan, J., Zhang, Q., Li, J., Beck, M. J., Xiao, X., and Cheng, Y. T., 2015, "Effects of Stress on Lithium Transport in Amorphous Silicon Electrodes for Lithium-Ion Batteries," Nano Energy, **13**, pp. 192–199.
[47] Choi, Y. M., and Pyun, S. I., 1997, "Effects of Intercalation-Induced Stress on Li Transport Through Porous $LiCoO_2$ Electrode," Solid State Ionics, **99**(3), pp. 173–183.
[48] Prussin, S., 1961, "The Generation and Distribution of Dislocations by Solute Diffusion," J. Appl. Phys., **32**(10), p. 1876.
[49] Larche, F., and Cahn, J. W., 1973, "Linear Theory of Thermochemical Equilibrium of Solids Under Stress," Acta Metall., **21**(8), pp. 1051–1063.
[50] Larche, F., and Cahn, J. W., 1978, "Non-Linear Theory of Thermochemical Equilibrium of Solids Under Stress," Acta Metall., **26**(1), pp. 53–60.
[51] Li, J. C. M., 1978, "Physical-Chemistry of Some Microstructural Phenomena," Metall. Mater. Trans. A, **9**(10), pp. 1353–1380.
[52] Stephenson, G. B., 1988, "Deformation During Interdiffusion," Acta Metall., **36**(10), pp. 2663–2683.
[53] Christensen, J., and Newman, J., 2006, "Stress Generation and Fracture in Li Insertion Materials," J. Solid State Electrochem., **10**(5), pp. 293–319.
[54] Christensen, J., and Newman, J., 2006, "A Mathematical Model of Stress Generation and Fracture in Li Manganese Oxide," J. Electrochem. Soc., **153**(6), pp. A1019–A1030.
[55] Zhang, X. C., Shyy, W., and Sastry, A. M., 2007, "Numerical Simulation of Intercalation-Induced Stress in Li-Ion Battery Electrode Particles," J. Electrochem. Soc., **154**(10), pp. A910–A916.
[56] Zhang, X. C., Sastry, A. M., and Shyy, W., 2008, "Intercalation-Induced Stress and Heat Generation Within Single Li-Ion Battery Cathode Particles," J. Electrochem. Soc., **155**(7), pp. A542–A552.
[57] Golmon, S., Maute, K., Lee, S. H., and Dunn, M. L., 2010, "Stress Generation in Silicon Particles During Li Insertion," Appl. Phys. Lett., **97**(3), p. 033111.
[58] Cheng, Y. T., and Verbrugge, M. W., 2009, "Evolution of Stress Within a Spherical Insertion Electrode Particle Under Potentiostatic and Galvanostatic Operation," J. Power Sources, **190**(2), pp. 453–460.
[59] Cheng, Y. T., and Verbrugge, M. W., 2010, "Diffusion-Induced Stress, Interfacial Charge Transfer, and Criteria for Avoiding Crack Initiation of Electrode Particles," J. Electrochem. Soc., **157**(4), pp. A508–A516.
[60] Haftbaradaran, H., Gao, H. J., and Curtin, W. A., 2010, "A Surface Locking Instability for Atomic Intercalation Into a Solid Electrode," Appl. Phys. Lett., **96**(9), p. 091909.
[61] Haftbaradaran, H., Song, J., Curtin, W. A., and Gao, H. J., 2011, "Continuum and Atomistic Models of Strongly Coupled Diffusion, Stress, and Solute Concentration," J. Power Sources, **196**(1), pp. 361–370.
[62] Gao, Y. F., and Zhou, M., 2012, "Strong Dependency of Li Diffusion on Mechanical Constraints in High-Capacity Li-Ion Battery Electrodes," Acta Mech. Sin., **28**(4), pp. 1068–1077.
[63] Cheng, Y. T., and Verbrugge, M. W., 2008, "The Influence of Surface Mechanics on Diffusion Induced Stresses Within Spherical Nanoparticles," J. Appl. Phys., **104**(8), p. 083521.
[64] DeLuca, C. M., Maute, K., and Dunn, M. L., 2011, "Effects of Electrode Particle Morphology on Stress Generation in Silicon During Li Insertion," J. Power Sources, **196**(22), pp. 9672–9681.
[65] Deshpande, R., Cheng, Y. T., and Verbrugge, M. W., 2010, "Modeling Diffusion-Induced Stress in Nanowire Electrode Structures," J. Power Sources, **195**(15), pp. 5081–5088.
[66] Garcia, R. E., Chiang, Y. M., Carter, W. C., Limthongkul, P., and Bishop, C. M., 2005, "Microstructural Modeling and Design of Rechargeable Li-Ion Batteries," J. Electrochem. Soc., **152**(1), pp. A255–A263.
[67] Purkayastha, R. T., and McMeeking, R. M., 2012, "An Integrated 2-D Model of a Li Ion Battery: The Effect of Material Parameters and Morphology on Storage Particle Stress," Comput. Mech., **50**(2), pp. 209–227.
[68] Zhang, J. Q., Lu, B., Song, Y. C., and Ji, X., 2012, "Diffusion Induced Stress in Layered Li-Ion Battery Electrode Plates," J. Power Sources, **209**, pp. 220–227.
[69] Yang, B., He, Y. P., Irsa, J., Lundgren, C. A., Ratchford, J. B., and Zhao, Y. P., 2012, "Effects of Composition-Dependent Modulus, Finite Concentration and Boundary Constraint on Li-Ion Diffusion and Stresses in a Bilayer Cu-Coated Si Nano-Anode," J. Power Sources, **204**, pp. 168–176.
[70] Lim, C., Yan, B., Yin, L. L., and Zhu, L. K., 2012, "Simulation of Diffusion-Induced Stress Using Reconstructed Electrodes Particle Structures Generated by Micro/Nano-CT," Electrochim. Acta, **75**, pp. 279–287.
[71] Huang, H. Y. S., and Wang, Y. X., 2012, "Dislocation Based Stress Developments in Li-Ion Batteries," J. Electrochem. Soc., **159**(6), pp. A815–A821.
[72] Bhandakkar, T. K., and Johnson, H. T., 2012, "Diffusion Induced Stresses in Buckling Battery Electrodes," J. Mech. Phys. Solids, **60**(6), pp. 1103–1121.
[73] Barai, P., and Mukherjee, P. P., 2013, "Stochastic Analysis of Diffusion Induced Damage in Lithium-Ion Battery Electrodes," J. Electrochem. Soc., **160**(6), pp. A955–A967.
[74] Chen, C. F., Barai, P., and Mukherjee, P. P., 2014, "Diffusion Induced Damage and Impedance Response in Lithium-Ion Battery Electrodes," J. Electrochem. Soc., **161**(14), pp. A2138–A2152.
[75] Barai, P., and Mukherjee, P. P., 2016, "Mechano-Electrochemical Stochastics in High-Capacity Electrodes for Energy Storage," J. Electrochem. Soc., **163**(6), pp. A1120–A1137.
[76] Bower, A. F., Guduru, P. R., and Sethuraman, V. A., 2011, "A Finite Strain Model of Stress, Diffusion, Plastic Flow, and Electrochemical Reactions in a Lithium-Ion Half-Cell," J. Mech. Phys. Solids, **59**(4), pp. 804–828.
[77] Di Leo, C. V., Rejovitzky, E., and Anand, L., 2015, "Diffusion–Deformation Theory for Amorphous Silicon Anodes: The Role of Plastic Deformation on Electrochemical Performance," Int. J. Solids Struct., **67–68**, pp. 283–296.
[78] Zhao, K., Pharr, M., Vlassak, J. J., and Suo, Z., 2011, "Inelastic Hosts as Electrodes for High-Capacity Lithium-Ion Batteries," J. Appl. Phys., **109**(1), p. 016110.
[79] Brassart, L., Zhao, K., and Suo, Z., 2013, "Cyclic Plasticity and Shakedown in High-Capacity Electrodes of Lithium-Ion Batteries," Int. J. Solids Struct., **50**(7), pp. 1120–1129.
[80] Cui, Z., Gao, F., and Qu, J., 2012, "A Finite Deformation Stress-Dependent Chemical Potential and Its Applications to Lithium Ion Batteries," J. Mech. Phys. Solids, **60**(7), pp. 1280–1295.
[81] Xu, R., and Zhao, K., 2015, "Mechanical Interactions Regulated Kinetics and Morphology of Composite Electrodes in Li-Ion Batteries," Extreme Mech. Lett., **8**, pp. 13–21.
[82] Verbrugge, M. W., and Koch, B. J., 1996, "Modeling Li Intercalation of Single-Fiber Carbon Microelectrodes," J. Electrochem. Soc., **143**(2), pp. 600–608.
[83] Karthikeyan, D. K., Sikha, G., and White, R. E., 2008, "Thermodynamic Model Development for Li Intercalation Electrodes," J. Power Sources, **185**(2), pp. 1398–1407.
[84] Sethuraman, V. A., Srinivasan, V., Bower, A. F., and Guduru, P. R., 2010, "In Situ Measurements of Stress-Potential Coupling in Lithiated Silicon," J. Electrochem. Soc., **157**(11), pp. A1253–A1261.
[85] Piper, D. M., Yersak, T. A., and Lee, S. H., 2013, "Effect of Compressive Stress on Electrochemical Performance of Silicon Anodes," J. Electrochem. Soc., **160**(1), pp. A77–A81.
[86] Lu, B., Song, Y., Zhang, Q., Pan, J., Cheng, Y. T., and Zhang, J., 2016, "Voltage Hysteresis of Lithium Ion Batteries Caused by Mechanical Stress," Phys. Chem. Chem. Phys., **18**(6), pp. 4721–4727.
[87] Kim, S., Choi, S. J., Zhao, K., Yang, H., Gobbi, G., Zhang, S., and Li, J., 2016, "Electrochemically Driven Mechanical Energy Harvesting," Nat. Commun., **7**, p. 10146.
[88] Chon, M. J., Sethuraman, V. A., McCormick, A., Srinivasan, V., and Guduru, P. R., 2011, "Real-Time Measurement of Stress and Damage Evolution During Initial Lithiation of Crystalline Silicon," Phys. Rev. Lett., **107**(4), p. 045503.
[89] Liu, X. H., Zheng, H., Zhong, L., Huang, S., Karki, K., Zhang, L. Q., Liu, Y., Kushima, A., Liang, W. T., Wang, J. W., Cho, J.-H., Epstein, E., Dayeh, S. A.,

Picraux, S. T., Zhu, T., Li, J., Sullivan, J. P., Cumings, J., Wang, C., Mao, S. X., Ye, Z. Z., Zhang, S., and Huang, J. Y., 2011, "Anisotropic Swelling and Fracture of Silicon Nanowires During Lithiation," Nano Lett., **11**(8), pp. 3312–3318.
[90] Yang, H., Fan, F., Liang, W., Guo, X., Zhu, T., and Zhang, S., 2014, "A Chemo-Mechanical Model of Lithiation in Silicon," J. Mech. Phys. Solids, **70**, pp. 349–361.
[91] Limthongkul, P., Jang, Y. I., Dudney, N. J., and Chiang, Y. M., 2003, "Electrochemically-Driven Solid-State Amorphization in Lithium–Silicon Alloys and Implications for Lithium Storage," Acta Mater., **51**(4), pp. 1103–1113.
[92] McDowell, M. T., Lee, S. W., Wang, C., Nix, W. D., and Cui, Y., 2012, "Studying the Kinetics of Crystalline Silicon Nanoparticle Lithiation With In Situ Transmission Electron Microscopy," Adv. Mater., **24**(45), pp. 6034–6041.
[93] Zhang, Y., Li, Y., Wang, Z., and Zhao, K., 2014, "Lithiation of SiO_2 in Li-Ion Batteries: In Situ Transmission Electron Microscopy Experiments and Theoretical Studies," Nano Lett., **14**(12), pp. 7161–7170.
[94] Liu, D. J., Weeks, J. D., and Kandel, D., 1998, "Current-Induced Step Bending Instability on Vicinal Surfaces," Phys. Rev. Lett., **81**(13), p. 2743.
[95] Nielsen, J. F., Pelz, J. P., and Pettersen, M. S., 2000, "Observation of Direct-Current-Induced Step Bending Patterns on Si (001)," Surf. Rev. Lett., **7**(5–6), pp. 577–582.
[96] Zhang, Y., Wang, Z., Li, Y., and Zhao, K., 2015, "Lithiation of ZnO Nanowires Studied by In Situ Transmission Electron Microscopy and Theoretical Analysis," Mech. Mater., **91**(Pt. 2), pp. 313–322.
[97] Jia, Z., and Li, T., 2016, "Intrinsic Stress Mitigation Via Elastic Softening During Two-Step Electrochemical Lithiation of Amorphous Silicon," J. Mech. Phys. Solids, **91**, pp. 278–290.
[98] Hertzberg, B., Benson, J., and Yushin, G., 2011, "Ex-Situ Depth-Sensing Indentation Measurements of Electrochemically Produced Si-Li Alloy Films," Electrochem. Commun., **13**(8), pp. 818–821.
[99] Ratchford, J. B., Crawford, B. A., Wolfenstine, J., Allen, J. L., and Lundgren, C. A., 2012, "Young's Modulus of Polycrystalline $Li_{12}Si_7$ Using Nanoindentation Testing," J. Power Sources, **211**, pp. 1–3.
[100] Levitas, V. I., and Attariani, H., 2013, "Anisotropic Compositional Expansion and Chemical Potential for Amorphous Lithiated Silicon Under Stress Tensor," Sci. Rep., **3**, p. 1615.
[101] Levitas, V. I., and Attariani, H., 2014, "Anisotropic Compositional Expansion in Elastoplastic Materials and Corresponding Chemical Potential: Large-Strain Formulation and Application to Amorphous Lithiated Silicon," J. Mech. Phys. Solids, **69**, pp. 84–111.
[102] Hong, W., 2015, "A Kinetic Model for Anisotropic Reactions in Amorphous Solids," Extreme Mech. Lett., **2**, pp. 46–51.
[103] Khosrownejad, S. M., and Curtin, W. A., 2016, "Model for Charge/Discharge-Rate-Dependent Plastic Flow in Amorphous Battery Materials," J. Mech. Phys. Solids, **94**, pp. 167–180.
[104] Choi, J. W., Cui, Y., and Nix, W. D., 2011, "Size-Dependent Fracture of Si Nanowire Battery Anodes," J. Mech. Phys. Solids, **59**(9), pp. 1717–1730.
[105] Liu, X. H., Zhong, L., Huang, S., Mao, S. X., Zhu, T., and Huang, J. Y., 2012, "Size-Dependent Fracture of Silicon Nanoparticles During Lithiation," ACS Nano, **6**(2), pp. 1522–1531.
[106] Zhao, K., Pharr, M., Hartle, L., Vlassak, J. J., and Suo, Z., 2012, "Fracture and Debonding in Lithium-Ion Batteries With Electrodes of Hollow Core–Shell Nanostructures," J. Power Sources, **218**, pp. 6–14.
[107] Lee, S. W., Lee, H. W., Nix, W. D., Gao, H., and Cui, Y., 2015, "Kinetics and Fracture Resistance of Lithiated Silicon Nanostructure Pairs Controlled by Their Mechanical Interaction," Nat. Commun., **6**, p. 7533.
[108] Deshpande, R., Verbrugge, M., Cheng, Y. T., Wang, J., and Liu, P., 2012, "Battery Cycle Life Prediction With Coupled Chemical Degradation and Fatigue Mechanics," J. Electrochem. Soc., **159**(10), pp. A1730–A1738.
[109] Sethuraman, V. A., Chon, M. J., Shimshak, M., Van Winkle, N., and Guduru, P. R., 2010, "In Situ Measurement of Biaxial Modulus of Si Anode for Li-Ion Batteries," Electrochem. Commun., **12**(11), pp. 1614–1617.
[110] Vasconcelos, L. S., Xu, R., Li, J., and Zhao, K., 2016, "Grid Indentation Analysis of Mechanical Properties of Composite Electrodes in Li-Ion Batteries," Extreme Mech. Lett., **9**(Pt. 3), pp. 495–502.
[111] Qi, Y., Hector, L. G., James, C., and Kim, K. J., 2014, "Lithium Concentration Dependent Elastic Properties of Battery Electrode Materials From First Principles Calculations," J. Electrochem. Soc., **161**(11), pp. F3010–F3018.
[112] Shenoy, V. B., Johari, P., and Qi, Y., 2010, "Elastic Softening of Amorphous and Crystalline Li-Si Phases With Increasing Li Concentration: A First-Principles Study," J. Power Sources, **195**(19), pp. 6825–6830.
[113] Choi, Y. S., Pharr, M., Oh, K. H., and Vlassak, J. J., 2015, "A Simple Technique for Measuring the Fracture Energy of Lithiated Thin-Film Silicon Electrodes at Various Lithium Concentrations," J. Power Sources, **294**, pp. 159–166.
[114] Berla, L. A., Lee, S. W., Cui, Y., and Nix, W. D., 2014, "Robustness of Amorphous Silicon During the Initial Lithiation/Delithiation Cycle," J. Power Sources, **258**, pp. 253–259.
[115] Grantab, R., and Shenoy, V. B., 2012, "Pressure-Gradient Dependent Diffusion and Crack Propagation in Lithiated Silicon Nanowires," J. Electrochem. Soc., **159**(5), pp. A584–A591.
[116] Yang, H., Huang, X., Liang, W., Van Duin, A. C., Raju, M., and Zhang, S., 2013, "Self-Weakening in Lithiated Graphene Electrodes," Chem. Phys. Lett., **563**, pp. 58–62.
[117] Yang, F., Liu, B., and Fang, D. N., 2011, "Interplay Between Fracture and Diffusion Behaviors: Modeling and Phase Field Computation," Comput. Mater. Sci., **50**(9), pp. 2554–2560.
[118] Evans, A. G., Mumm, D. R., Hutchinson, J. W., Meier, G. H., and Pettit, F. S., 2001, "Mechanisms Controlling the Durability of Thermal Barrier Coatings," Prog. Mater. Sci., **46**(5), pp. 505–553.
[119] Xu, R., Fan, X. L., Zhang, W. X., and Wang, T. J., 2014, "Interfacial Fracture Mechanism Associated With Mixed Oxides Growth in Thermal Barrier Coating System," Surf. Coat. Technol., **253**, pp. 139–147.
[120] Klinsmann, M., Rosato, D., Kamlah, M., and McMeeking, R. M., 2016, "Modeling Crack Growth During Li Insertion in Storage Particles Using a Fracture Phase Field Approach," J. Mech. Phys. Solids, **92**, pp. 313–344.